Modelling and simulation of dynamic modes in manipulation of nanorods

M. H. Korayem, A. K. Hoshiar

Department of Mechanical and Aerospace Engineering, Science and Research Branch, Islamic Azad University, Tehran, Iran
E-mail: Hkorayem@iust.ac.ir

Published in Micro & Nano Letters; Received on 21st March 2013; Accepted on 17th April 2013

The use of atomic force microscopy (AFM)-based robots for moving cylindrical particles has become the focus of attention in recent research works. The impossibility of observing the moving process during motion has highlighted the role of computer simulation in the investigation of nanoparticles' movement. The motion modes (sliding, rolling, spinning) are used to investigate the mode by which a particle moves on a substrate. By using the presented model it is possible to simulate the conditions under which each of these modes are created. To validate the results, it has been observed that by gradual reduction of the nanorod's length, the obtained results are more similar to the results of the spherical case. Furthermore, the presented modes have been evaluated by comparing with the experimental findings, which shows adequate compatibility and acceptable accuracy. In this Letter, first, the movement of particles is modelled and then the effective parameters of the process are simulated. Afterwards, the simulation of dynamic modes is carried out and, finally, verification of the results is presented. By using the presented simulations, it would be possible to predict the mode of movement during the manipulation of nanorods by means of AFM nanorobots.

1. Introduction: Nowadays, the use of atomic force microscopy (AFM) nanorobots to manipulate and move micro/nanoparticles has attracted widespread attention. In these types of operations, the cantilever of AFM acts as a robot arm and pushes the target particles on a substrate. These operations can be performed in different modes (rolling, sliding, spinning). The way by which the cylindrical nanoparticles are induced to move by AFM nanorobots is investigated in this Letter.

Various experiments have investigated the behaviour of cylindrical particles' movement on a substrate. Shikawa and Tsukagoshi [1] first formed nanoscale structures by using AFM nanorobots to move and displace single-layer nanotubes. Yang *et al.* employed the AFM nanorobots in the tapping mode to move cylindrical particles on a surface. They devised an algorithm for this purpose to help them accomplish such an operation automatically [2]. Next, the researchers turned their attention to cutting and separating nanorods by this method [3]. The conducted experiments have investigated the mechanical properties, and the motion modes have not been of interest in these research works. Subsequently, with the expansion of the AFM nanorobots' role in the displacement of nanorods, the created motion modes have been studied experimentally.

Montelius and coworkers [4] have studied the displacement of nanowires by this method and have observed the different modes of motion. Falov has experimentally investigated the motion modes in the manipulation of nanotubes. He has used an AFM-based manipulator in various tests to study different motion modes and the effect of the position on which the pushing force is applied [5]. Chang and Hsu [6] have investigated the manipulation of nanowires and examined the spinning mode and its affectability of the location of applied force. In the presented research works, the motion modes have been studied experimentally and no mathematical model has been offered for computer simulation of motion in different modes.

The manipulation of nanoparticles using the AFM nanorobots, and the displacement of spherical particles was simulated for the first time by Sitti and Hashimoto [7]. Then, the modelling of the motion modes (rolling and sliding cases) was performed by Tafazzoli and Sitti [8]. Korayem and Zakeri [9] evaluated the effective parameters of the process and carried out a sensitivity analysis of the presented models. Also, Korayem *et al.* [10] studied the dimensional limitations of the particles that could be moved by this method. Daeinabi *et al.* [11] subsequently developed a dynamic model of motion for displacement of spherical particles by means of different cantilevers. The introduced modelling approaches have dealt with the displacement of spherical particles. Owing to the change of models as a result of changing the friction conditions, which are directly dependent on particle shape, the researchers developed other models for displacement of cylindrical particles.

The manipulation of cylindrical particles has been modelled by Lianqing *et al.* This model has focused on the displacement of nanotubes on an electrode by pushing, which is implemented through an AFM nanorobot [12, 13]. Chen *et al.* [14] have attempted to present an exact method for moving and displacing nanotubes on a surface and to form certain structures on the surface through controlled manipulation by using an algorithm. Li *et al.* [15] have investigated the manipulation of nanotubes and nanowires by using the AFM; and by examining the resultant friction and the governing conditions of the motion and also by considering the locations where the forces are applied, they have studied the manipulation process. The critical time and force of movement in the displacement of cylindrical particles using the AFM robot have been investigated by Moradi *et al.* [16]; in his paper, the critical time and force of the movement have been simulated by assuming a disc model for the nanorods and taking the sliding and rolling modes into consideration. The presented models have not considered all of the three motion modes (sliding, rolling, spinning). Also, in these approaches, the disc model has been used for studying the motion mode, and no comprehensive model, which expresses the manner of movement in three-dimensional format by using the cylindrical model, has been presented.

The main goal of this Letter is to present a model that can be used to determine the necessary forces for the start of each motion mode in the displacement of nanorods. First, a model has been specified for expressing each of the motion conditions and then the effect of different parameters has been investigated. Subsequently, the dynamic conditions that emerge during the displacement of nanorods have been simulated and finally, the results have been compared with previous theoretical and experimental findings.

2. Modelling of motion modes: Dynamic modes for a spherical nanoparticle have been widely investigated by Korayem and Zakeri [9]. Sliding and rolling modes in the manipulation of cylindrical nanoparticles are similar to spherical nanoparticles. However, the main dynamic mode, which is spinning, only occurs in nanorod manipulation. Moreover, the contact mechanism for nanorods is different from spherical nanoparticle contact [17, 18].

© The Institution of Engineering and Technology 2013

doi: 10.1049/mnl.2013.0162

In this Section, the motion modes in displacement of nanorods by AFM nanorobots have been examined. For this purpose, first, the forces exerted on the nanoparticle are plotted, and then by considering the equilibrium point, different motion models are presented. In general, two groups of forces are observed in Fig. 1. The first group which includes the forces exerted by the probe tip on the nanoparticle (F_X, F_Y, F_Z) and their resultants are the input forces, and the second group comprises those reaction forces produced at the point of contact between the probe tip and nanoparticle and also between the substrate and the nanoparticle, which have been designated by indices T and S, respectively. It should be noted that the contact and friction forces between the substrate and the nanoparticle have been taken as distributed forces.

In Fig. 1, the probe's head which is in direct contact with the nanoparticle is represented as a sphere. The pushing process causes deformations in different directions, which are shown in Fig. 1.

Taking Fig. 1 into consideration and using the forces and presented geometrical relations, the following equations are offered to specify the critical conditions for motion modes:

1. The sliding of the probe tip on the particle along the first direction

$$F^*_{\mathrm{Sl}_1} = \frac{\tau_{\mathrm{T}} A_{\mathrm{T}}}{\cos\varepsilon + \mu_{\mathrm{T}} \cos\varepsilon} \tag{1}$$

2. The sliding of the particle on the substrate

$$F^*_{\mathrm{S}} = \frac{\tau_{\mathrm{S}} A_{\mathrm{S}}}{\sin\psi_1 - \mu_{\mathrm{S}} \cos\psi_1} \tag{2}$$

3. The rolling of the particle on the substrate

$$F^*_{\mathrm{R}} = \frac{\tau_{r\mathrm{S}} A_{\mathrm{S}} + \tau_{r\mathrm{T}} A_{\mathrm{T}}}{R(\cos\varepsilon + \sin\psi_1) - \mu_{r\mathrm{S}} \cos\psi_1 + \mu_{r\mathrm{T}} \sin\varepsilon} \tag{3}$$

4. The sliding of the probe tip on the particle along the second direction

$$F^*_{\mathrm{Sl}_2} = \frac{\tau_{\mathrm{T}} A_{\mathrm{T}}}{\cot\psi_2 \cos\psi_1 + \mu_{\mathrm{T}} \sin\varepsilon} \tag{4}$$

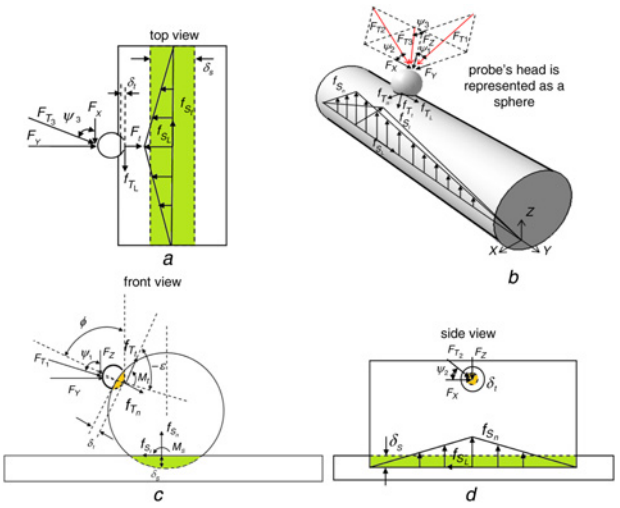


Figure 1 *Forces, moments and deformations produced during the manipulation of cylindrical particles*
a Top view
b Probe's head
c Front view
d Side view

5. The spinning of the particle on the substrate

$$F^*_{\mathrm{SP}} = \frac{\tau_{r\mathrm{S}} A_{\mathrm{S}} + \tau_{r\mathrm{T}} A_{\mathrm{T}}}{\cos\psi_1((4X - 2L)/3) + R\sin\psi_1 \cot\psi_3 - \mu_{r\mathrm{S}} \cos\psi_1 + \mu_{r\mathrm{T}} \sin\varepsilon} \tag{5}$$

According to (1)–(5), $F^*_{\mathrm{Sl}_1}$, F^*_{S}, F^*_{R}, $F^*_{\mathrm{Sl}_2}$ and F^*_{SP} are functions of pushing force angle ψ, probe particle contact angle ϕ, friction constants μ and τ, contact area A, particle's radius R and length L and the contact location X. Now, it is possible to determine the exact value of different dynamic modes.

The pushing force angle between F_Y and F_Z has been shown as ψ_1; also the angle between F_{T_1} and f_{T_t} has been introduced as ε. Based on geometrical relations, the dynamic parameters ψ_1 and ε have been introduced as:

$$\psi_1 = \tan^{-1}\left(\frac{F_Y}{F_Z}\right) \tag{6}$$

$$\varepsilon = \psi_1 - \varphi - 90 \tag{7}$$

In the simulation Section, the above presented parameters have been introduced as constants. To determine the contact area between the particles and the probe tip (A_{t}), the same approach as for a spherical particle has been used [8, 9, 17, 18]. The equations developed by Barquins [17] and Dillared and Pocius [18] are used to determine the contact area between the particles and the substrate A_{S}.

$$P = \frac{3\pi K a^2 L}{8R} - \sqrt{6\pi w K a L^2} \tag{8}$$

In the given equation, a is half the width of the contact zone, which is obtained by solving the presented equation and considering the applied force and the rest of the simulation parameters. In these equations, to specify the equivalent radius R, the particle radius has been considered almost equal to the equivalent radius; K denotes the equivalent coefficient of elasticity, L represents the length of the nanorod, w is the surface energy and P specifies the applied normal force. By using the presented equations, half of the width of the contact region (a) is determined. Finally, both the contact areas are obtained [8, 9].

3. Simulation of motion modes in manipulation of cylindrical particles: At this point, motion modes in the displacement of cylindrical particles using AFM nanorobots are explored and simulated. Five motion modes exist in the displacement of the nanorods [5, 6]. Two of these modes in fact represent a lack of movement (sliding of the probe tip over the particle) and the other three modes exhibit sliding, rolling and spinning of the nanorod.

At this stage, by using Table 1, constant parameters are determined for the simulation. Considering the relation between ε and ψ_1, the value of ψ_1 has been assumed as a variable in the range of 1°–360°, and thus, ε is specified in the interval between −9° and 350°. It should be mentioned that ψ_2 has been considered with a phase difference of 90°, and ψ_3 has been determined based on the geometrical relation between ψ_1, ψ_2 and ψ_3. Now, by considering the above-mentioned statements and using Table 1 to input the simulation constants, the required forces for the initiation of each motion mode can be simulated.

As is clear from Fig. 2, the possibility of establishing the sliding modes on the probe tip and aborting the manipulation operation for the mentioned conditions is higher for the lower forces with respect to the other modes. As has been considered in the motion modes of spherical nanoparticles [8, 9], these sliding modes are ignored in the dynamic state; and by establishing the right conditions in operation parameters, we would observe diminishing of their effects and accomplishment of the manipulation procedure. Considering the

© The Institution of Engineering and Technology 2013

Table 1 Constant parameters in the simulation of motion modes

process parameters	contact angle (ϕ)		contact location (X)	
	initial	final	initial	final
	10°	60°	0.75	0.9
geometrical parameters	length of nanoparticle (L)		radius of nanoparticle (R)	
	initial	final	initial	final
	1 μm	0.1 μm	20 nm	100 nm
substrate parameters	surface energy (ω), J/m^2		surface adhesion (τ), MPa	surface friction (μ)
	initial	final	28	0.8
	0.2	2		

process conditions and presented simulation, it is observed that the possibility of sliding motion mode is higher than the other two modes, and also the spinning and rolling motion modes are created close to each other.

At this stage, to explore the impact of various effective parameters, each of these parameters is changed from initial values to its final values specified in Table 1, and the results are examined. Based on the results for different cases, it can be concluded that the most effective parameter is the nanoparticle radius, as shown in Fig. 2.

At this stage, the motion modes have been simulated in the dynamic state, and the parameters that affect them have been reviewed. For particles with radius of $R_p = 700$ nm and using the presented constants (Table 1 initial values), the three motion modes (sliding, rolling, spinning) for cylindrical particles can be simulated according to Fig. 3. The presented simulation demonstrates how the cylindrical particle moves with regards to the geometrical specifications and the properties of the substrate, and it also indicates which motion mode has a higher probability of occurrence. As can be observed from Fig. 3, the spinning motion mode, which has been specified in the dynamic case, has the highest chance of occurrence. Now, the effect of particle size reduction is examined. As Fig. 3 shows, by reduction of particle radius to $R_p = 300$ nm, the spinning motion mode shifts to the right side, and it is not the effective mode. The other modes display severe changes, indicating an increase in the sliding mode's probability of occurrence under these circumstances.

Now, the effect of nanoparticle length on dynamic motion modes will be studied. Using the initial values of Table 1 and changing nanorod length from 0.1 to 1 μm, Fig 4*a* is represented. Taking Fig. 4*a* into consideration, it is observed that increasing the nanorod's length has enhanced nanomanipulation forces (the

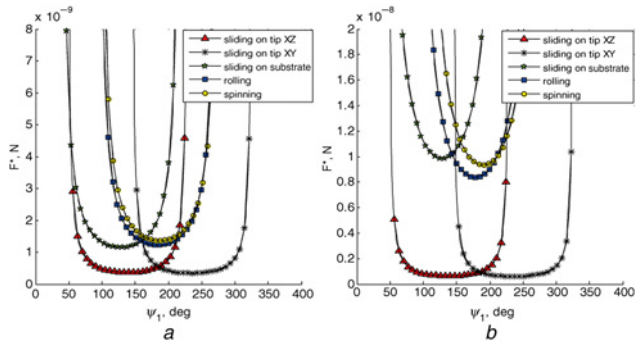


Figure 2 *Simulation of motion modes in the manipulation of nanorods*
a By using the values of Table 1 (initial values) (left side)
b By increasing the radius by the amount specified in Table 1 (final value) and using initial values for the rest of the parameters (right side)

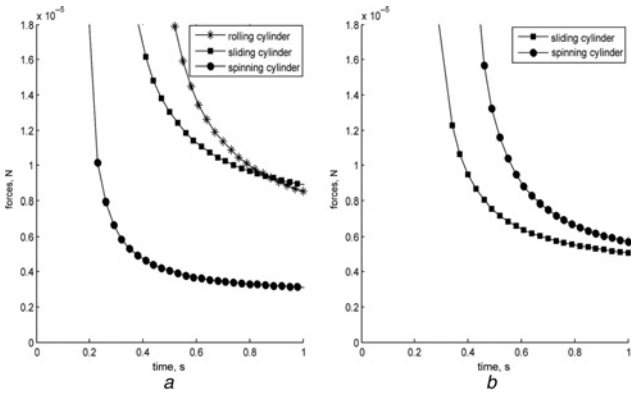


Figure 3 *Simulation of motion modes in the dynamic state*
a For particles with radius $R_p = 400$ nm (left side)
b For particles with radius $R_p = 300$ nm (right side)

case for sliding mode is similar). Both sliding and spinning forces have been increased by enhancement of the particle's length. However, the rate of force enhancement in the sliding mode is higher than the spinning mode (Fig. 4*b*). Therefore the spinning mode for particles with long length has a higher chance of occurrence.

To evaluate the validity of the presented simulations, first, the simulations of the rolling modes are examined (the result for sliding could be evaluated similarly). It is observed that with gradual reduction of the nanoparticle length with a constant diameter, the two simulations start to match up; and as can be seen in Fig. 5, for particles with a diameter of 700 nm and length of 30 nm (disc-shaped) and applying Table 1 information (initial values), both simulations' results are compatible with each other, and the discrepancy between the two simulations is due to the differences between cylindrical [17, 18] and spherical contact areas [8, 9].

In experimental approaches, nanorods have been pushed by the probe's tip [6]. The substance moves with a constant velocity during the process. In the first stage, the probe's tip impacts the particle. Meanwhile, a deformation in the cantilever occurs. In this phase, probe and particle are attached. However, the particle is stuck to the surface. Hence, manipulation forces increase (static phase). By the time that the particle starts to move by one of the described modes (spinning, sliding, rolling), the manipulation force reaches its peak (start of dynamic phase) [8, 9]. For a particle with 4.2 μm length and 100 nm radius which has been pushed by a constant velocity of 0.1 μm, a real-time LFM diagram is demonstrated in Fig. 6 [6]. By a domain change from displacement to

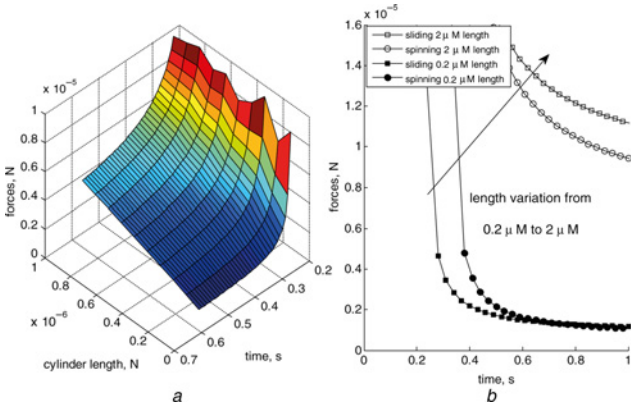


Figure 4 *Effect of particle's length*
a Simulation of spinning mode for particles with lengths from 100 to 1000 nm (left side)
b Shifting dynamic mode from sliding to spinning by variation of particle's lengths from 0.2 to 0.2 μm (right side)

© The Institution of Engineering and Technology 2013

doi: 10.1049/mnl.2013.0162

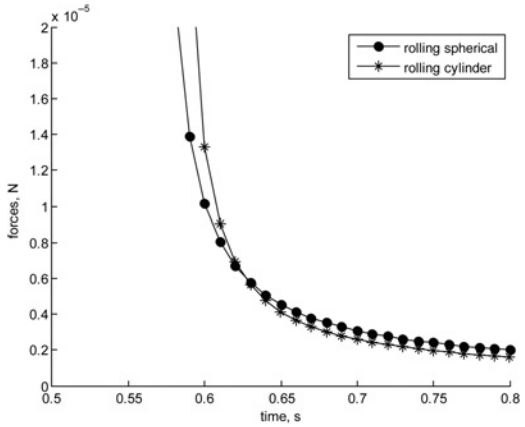


Figure 5 *Discrepancy between the rolling motion modes in cylindrical (disc-shaped particles with a radius of 700 nm and length of 30 nm) and spherical (radius of 700 nm) cases*

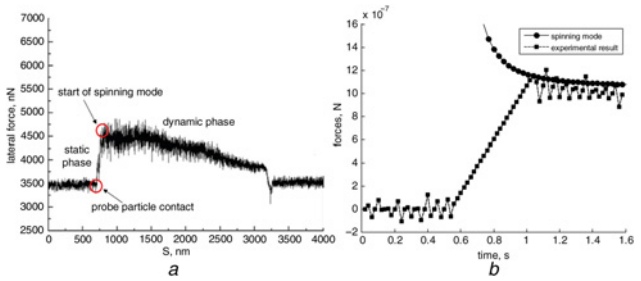


Figure 6 *Experimental result for nanorod manipulation*
a Real-time lateral force microscopy diagram [6] for $R_p = 100$ nm and $L = 4.2$ μm
b Simulation of the manipulation process in experimental setting [6] and its comparison with the presented simulation using Table 1 initial values and $R_p = 100$ nm and $L = 4.2$ μm

time (taking constant velocity into consideration), the motion mode which is shown in Fig. 6 is similar to the experimental results (reaches the same value and demonstrates the same dynamic mode which is spinning in this case); and the presented mode has correctly demonstrated the type of motion and its critical time.

4. Conclusion: As the presented simulations here demonstrated, the most effective parameter is the nanoparticle radius, by which increasing it from 20 to 100 nm, large increases can be observed in the necessary forces for initiation of sliding, rolling and spinning motion modes from about 2×10^{-9} to 1×10^{-8} N. This severe change confirms the high impact of geometrical parameters on motion modes. Also, in this Letter, the motion modes have been dynamically investigated. As the presented simulations indicated, the spinning mode occurs under the majority of circumstances, which confirms the findings of experimental reports. Under certain conditions, by reduction of the particle diameter and the particle length, it is observed that the motion mode has changed from spinning to sliding. Also, by reduction of the nanoparticle length, the rolling mode can be observed under particular friction conditions.

Using the model presented in this Letter, it is observed that for particles with small radius ($R_p = 100$ nm) and short length ($L = 0.1$ μm), and considering the presented substrate characteristics, the sliding motion mode has a higher chance of occurrence rather than the spinning mode whereas by increasing the particle diameter ($R_p = 700$ nm) or the particle length ($L = 1$ μm), the spinning mode has a higher probability of occurrence with respect to the sliding mode, which indicates the impact of predicting the particular mode which is created during the displacement of a nanoparticle.

5 References

[1] Shikawa T., Tsukagoshi K.: 'Nanostructure construction in single-walled carbon nanotube by AFM manipulation'. IEEE Microprocesses and Nanotechnology Conf., 2001, pp. 164–165
[2] Yang Y., Dong Z., Qu Y., Li M., Li W.J.: 'A programmable AFM-based nanomanipulation method using vibration-mode operation'. IEEE Int. Conf. Nano/Micro Engineered and Molecular Systems, 2008, pp. 681–685
[3] Shen Z., Liu S., Hou S., Xue Z.: 'Manipulation of carbon nanotube bundles with contact mode atomic force microscopy', *Int. J. Nanosci.*, 2002, **1**, pp. 575–579
[4] Conache G., Gray S., Bordag M., *ET AL.*: 'AFM-based manipulation of InAs nanowires', *J. Phys., Conf. Ser.*, 2008, **100**, pp. 052051–052054
[5] Falov M.: 'Studies of the mechanics and friction of nanometer-scale materials'. Ph.D. thesis, 1997, pp. 60–105
[6] Hsu J.H., Chang S.H.: 'Tribological interaction between multi-walled carbon nanotubes and silica surface using lateral force microscopy', *Wear*, 2009, **266**, pp. 952–959
[7] Sitti M., Hashimoto H.: 'Controlled pushing of nanoparticles: modeling and experiments', *IEEE/ASME Trans. Mechatronics*, 2000, **5**, pp. 199–211
[8] Tafazzoli A., Sitti M.: 'Dynamic modes of nanoparticle motion during nanoprobe-based manipulation'. IEEE Nanotechnology Conf., 2004, pp. 35–37
[9] Korayem M.H., Zakeri M.: 'Sensitivity analysis of nanoparticles pushing critical conditions in 2-D controlled nanomanipulation based on AFM', *Int. J. Adv. Manuf. Technol.*, 2009, **41**, pp. 714–726
[10] Korayem M.H., Hoshiar A.K., Ebrahimi N.: 'Maximum allowable load of atomic force microscope (AFM) nanorobot', *Int. J. Adv. Manuf. Technol.*, 2009, **43**, pp. 690–700
[11] Daeinabi K., Korayem M.H., Yarijani S.A.: 'Spring constant analysis of the AFM rectangular, V-shaped and dagger cantilever probes', *Micro Nano Lett.*, 2011, **6**, pp. 1007–1011
[12] Lianqing L., Peng Y., Xiaojun T., Yuechao W., Zaili D., Ning X.: 'Force analysis of top-down forming CNT electrical connection using nanomanipulation robot'. Int. Conf. Mechatronics and Automation, 2006, pp. 113–117
[13] Lai K.W.C., Xi N., Fung C.K.M., *ET AL.*: 'Automated nanomanufacturing system to assemble carbon nanotube based devices', *Int. J. Robot. Res.*, 2009, **28**, pp. 465–467
[14] Chen H., Xi N., Li G., Zhang J., Prokos M.: 'Planning and control for automated nanorobotic assembly'. IEEE Int. Conf. Robotics and Automation, 2005, pp. 169–174
[15] Li G., Xi N., Chen H., Saeed A., Yu M.: 'Assembly of nanostructure using AFM based nanomanipulation system'. IEEE Int. Conf. Robotics and Automation, 2004, pp. 428–433
[16] Moradi M., Fereidon A.H., Sadeghzadeh S.: 'Aspect ratio and dimension effects on nanorod manipulation by atomic force microscope', *Micro Nano Lett.*, 2010, **5**, pp. 324–327
[17] Barquins M.: 'Adherence and rolling kinetics of a rigid cylinder in contact with a natural rubber surface', *J. Adhes.*, 1988, **26**, pp. 1–12
[18] Dillared D.A., Pocius A.V.: 'The mechanism of adhesion' (Elsevier Science, 2002), pp. 88–92

© The Institution of Engineering and Technology 2013